Graphene oxide paper as a saturable absorber for Er- and Tm-doped fiber lasers

Jakub Boguslawski,[1,*] Jaroslaw Sotor,[1] Grzegorz Sobon,[1] Rafal Kozinski,[2] Krzysztof Librant,[2] Magdalena Aksienionek,[2] Ludwika Lipinska,[2] and Krzysztof M. Abramski[1]

[1]*Laser & Fiber Electronics Group, Wroclaw University of Technology, Wybrzeze Wyspianskiego 27, 50-370 Wroclaw, Poland*

[2]*Institute of Electronic Materials Technology, Wolczynska 133, 01-919 Warsaw, Poland*

**Corresponding author: jakub.boguslawski@pwr.edu.pl*

Received January 6, 2015; revised April 9, 2015; accepted April 9, 2015; posted April 15, 2015 (Doc. ID 231568); published May 18, 2015

In this work pulse generation in both the 1.5 and 2 μm spectral ranges using a graphene oxide (GO)-paper-based saturable absorber in Er- and Tm-doped fiber lasers is presented. The article describes the fabrication method of GO paper and its characterization. The performance of both lasers is discussed in detail. Stable, mode-locked operation provides 613 fs and 1.36 ps soliton pulses centered at 1565.9 and 1961.6 nm in Er- and Tm-doped fiber lasers, respectively. Furthermore, scaling of spectral width, and hence the pulse duration, by increasing the number of GO paper layers in the Er-doped laser is described. The versatility and simplicity of GO paper fabrication combined with the possibility of scaling the optical spectrum full width at half-maximum are essential features that make it a good candidate for ultrafast low-power mode-locked lasers operating in different spectral regions.

OCIS codes: (140.4050) Mode-locked lasers; (140.3510) Lasers, fiber; (060.3510) Lasers, fiber; (160.4236) Nanomaterials; (160.4330) Nonlinear optical materials.

http://dx.doi.org/10.1364/PRJ.3.000119

1. INTRODUCTION

Ultrafast fiber lasers are currently one of the most intensively developed branches of laser science and technology. Since they are compact, robust, and offer excellent beam quality, fiber-based devices are considered an interesting alternative for solid-state lasers. Among many techniques for inducing mode-locking operation, the most popular is the use of semiconductor saturable absorber mirrors (SESAMs) [1,2]. This solution, though a well-established technology, suffers from a complicated and expensive fabrication process. A narrow operation bandwidth is yet another limitation. Another way to achieve mode-locking operation is to use nonlinear polarization evolution (NPE), which enables generation of the shortest pulses [3]; however, it is environmentally unstable and usually does not provide self-starting operation. For these reasons, new, more versatile materials for ultrashort pulse generation are constantly sought.

The application of carbon nanotubes in the role of saturable absorber (SA) has led to a new class of carbon-based SA materials [4]. Graphene, the main representative of this category, is very suitable for this kind of application thanks to its unique optical properties [5–7]. The saturable absorption effect [5] combined with a fast recovery time and wavelength-independent absorption [6,7] facilitate its usage as an efficient SA in Yb-doped [8,9], Er-doped [10–14], and Tm-doped fiber lasers [15–17]. The usage of graphene SAs allows also for ultrashort pulse generation in different spectral ranges simultaneously [18–20]. Carbon-based SAs were found to be efficient and versatile competitors for conventional SESAMs.

Graphene oxide (GO) is a material composed of carbon, oxygen, and hydrogen [21]. It has attracted a lot of attention due to its cost-effective fabrication method and prospects for mass production [22]. Similarly to graphene, it possesses saturable absorption in broad spectral range [23,24]. Various setups incorporating GO as a SA in fiber lasers have been presented [25–32]. Passive mode-locking operation was presented at 1 μm [25], 1.5 μm [26–29], and 2 μm spectral ranges [30], as well as *Q*-switching operation [31,32]. In our previous work we showed that GO is an efficient SA and there is no reason to perform complicated reduction of GO in order to obtain reduced graphene oxide (rGO) [28]. A chemically produced solution of GO can be deposited either on a fiber connector [25], a mirror [26,27], a fused silica flat-parallel plate [28], or a side-polished fiber [30]. In comparison to other carbon-based and to other emerging SA materials (like topological insulators and few-layer MoS_2 [33,34]), GO is characterized by high solubility, which translates into an effective and straightforward fabrication process that is suitable for mass production. Additionally, a material in a form of paper or foil simplifies the manufacturing process and creates the possibility to control the parameters of a SA.

Recently, a novel type of GO-based material was presented, namely, GO paper. A free-standing, black-brown paper-like material was prepared by flow-directed assembly of individual GO sheets [35]. GO paper is nonconductive and has exceptional mechanical properties at the same time [36]. Nevertheless, the optical properties of GO paper were somewhat neglected and have not been investigated very thoroughly. The first report on ultrashort pulse generation using GO paper as a SA has already been presented. Ismail *et al.* showed a 680 fs Er-doped fiber laser based on commercially available GO

paper, but high susceptibility to damage and short-time operation were major disadvantages [37].

Herein, we present ultrashort pulse generation in both Er- and Tm-doped fiber lasers using GO paper in the role of SA. Stable mode-locking operation was observed over a period of several hours. Further, the possibility of full width at half-maximum (FWHM) scaling in Er-doped fiber laser was shown. It is possible due to the development of thinner and much more uniform material than in [38]. Experiments proved that GO paper may be considered a universal and efficient material for ultrafast laser applications.

2. GRAPHENE OXIDE PAPER PREPARATION AND CHARACTERIZATION

GO was synthesized by the Marcano method from Asbury 1 flake graphite. Graphite was oxidized by potassium permanganate in a mixture of sulfuric and phosphoric acids. The reaction was carried out at 50°C for 8 h. Oxidation was terminated by pouring the reaction mixture onto deionized water ice, and the excess of oxidant was neutralized with 30% hydrogen peroxide. Graphite oxide (GtO) was pre-purified by sedimentation and then centrifuged. When the GtO suspension pH reached about 4, sonication was performed to exfoliate GtO into GO. Graphene paper was made through vacuum filtration. A 2 mL GO suspension with concentration of 15 mg/mL was homogenized on a vortex mixer. Then it was vacuum filtrated on a polyvinylidene difluoride (PVDF) 0.22 μm membrane. Dried semitransparent GO paper was easily peeled off the membrane.

A photograph of black-brown GO paper is presented in Fig. 1(a). Raman spectroscopy was performed to characterize the crystalline structure of graphene-based material [39]. The measurement was performed using a Renishaw inVia Raman Microscope (×50 VIS LWD objective) with a 532 nm Nd:YAG laser. No reduction of GO to rGO was observed during the measurement. The result is presented in Fig. 1(b). The sample has a typical GO Raman spectra. The G peak position is 1601 cm^{-1}, which is redshifted from graphite as a result of functional groups on both sides of the GO flakes. The D peak position value is closer to 1350 cm^{-1}, which means that chains of hydroxyl and epoxy groups are present. The ratio is equal to 0.93, which indicates that, for every six atoms of carbon, there is half of an epoxy group and two hydroxyl groups [40]. Scanning electron microscopy (SEM) was performed to determine the morphological structure of the sample. The surface of the GO paper is presented in Fig. 2(a). As indicated in Raman spectroscopy, GO paper is a few-layer material, which is clearly visible in the cross section shown in Fig. 2(b).

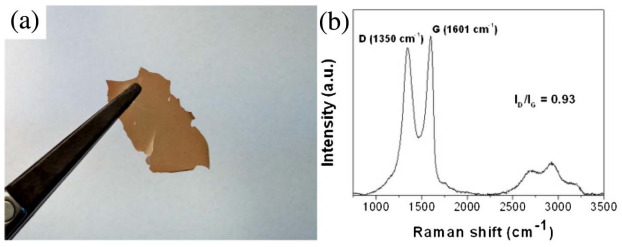

Fig. 1. (a) Photograph and (b) Raman spectrum of a GO paper sample.

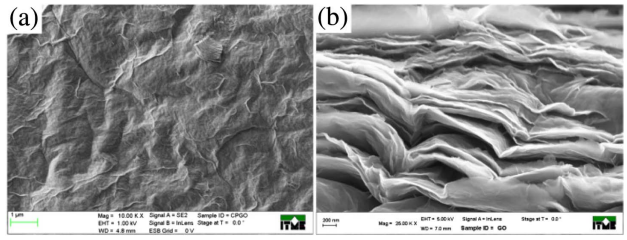

Fig. 2. SEM images of (a) GO paper surface with a 1 μm scale bar and (b) cross section with a 200 nm scale bar.

3. EXPERIMENTAL SETUP AND RESULTS

A. Er-Doped Fiber Laser

The experimental setup of an Er-doped fiber laser is schematically presented in Fig. 3. The laser consists of a 50 cm long active fiber (nLight Liekki Er80-4/125), a fiber isolator, an in-line polarization controller, a 980/1550 single-mode wavelength-division multiplexing coupler (WDM), through which a 980 nm pumping diode is connected, and a 20% output coupler. The total cavity length is 5.56 m. The net cavity dispersion is estimated to be −0.12 ps^2.

A small piece of GO paper was sandwiched between two fiber connectors to form a SA. The laser performance was observed with the use of an optical spectrum analyzer (Yokogawa AQ6370B), an autocorrelator (APE PulseCheck), a RF spectrum analyzer (Agilent EXA N9010A), and a digital oscilloscope (Agilent Infiniium DSO91304A) connected to a fast photodiode. No mode-locking operation was observed without the GO paper at any position of the polarization controller.

When a single layer of GO paper is placed between the fiber connectors, the laser starts to operate at continuous wave (CW) mode when the pump power exceeds 18 mW. The mode-locking operation starts when the pump power is set between the 23 and 52 mW and the polarization controller is properly set. No sign of CW lasing, modulation, or damage of the SA was observed at this interval of pumping power. The output spectrum with 1.7 nm FWHM is presented in Fig. 4 (black line with squares). When the next layers of GO paper were inserted, we observed broadening of the optical spectrum with each successive layer. The optical spectrum FWHM of the laser scaled up to 4.2 nm for four layers. The central wavelengths were slightly varying for each number of layers and are summarized in Table 1, together with other lasers' parameters. The

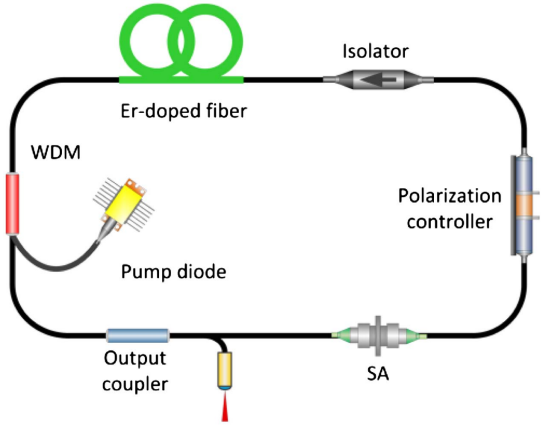

Fig. 3. Experimental setup of an Er-doped fiber laser.

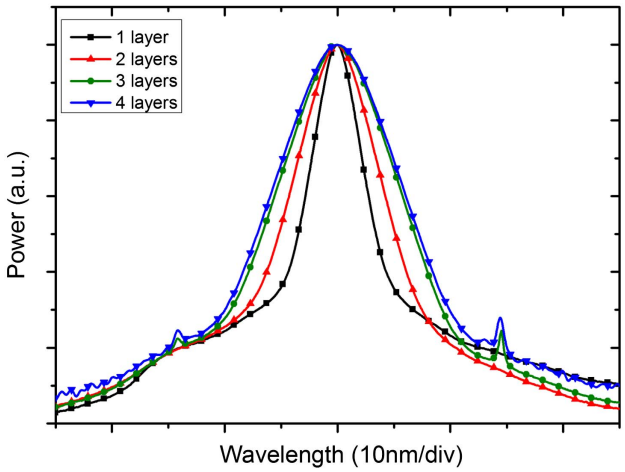

Fig. 4. The FWHM optical spectra comparison for Er-doped fiber laser with up to 4 layers of GO paper as a SA.

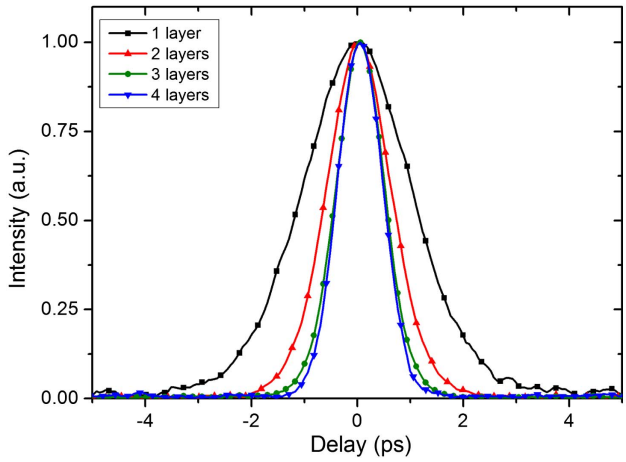

Fig. 5. Autocorrelation traces of output pulses from Er-doped fiber laser with up to 4 layers of GO paper as a SA.

comparison of optical spectra is depicted in Fig. 4 to illustrate scaling of the FWHM of output pulses. Along with broadening of the optical spectra, the autocorrelation traces of the output pulses have narrowed. Corresponding autocorrelation traces are presented in Fig. 5. Importantly, the time–bandwidth product (TBP) for each configuration was equal to 0.315, which means that pulses were transform-limited. Pulse duration was shortened from 1.53 ps for one layer to 613 fs for four layers, assuming the hyperbolic secant pulse shape proper for laser operating in the anomalous dispersion regime. The output RF spectrum of a laser working with one layer SA centered at a fundamental repetition rate of 37.2 MHz is presented in Fig. 6. The recorded spectrum with full available bandwidth up to 3 GHz is shown in the inset graph. The RF spectrum for each of the four configurations was identical, indicating stable mode-locking operation. The electrical signal-to-noise ratio (SNR) was ~70 dB. The average output powers, pulse energies, and peak powers are summarized in Table 1.

The power-dependent transmission characteristic of GO paper is presented in Fig. 7 together with the fitting curve according to the nonlinear transmission equation [38]. The measurement was performed in an all-fiber setup containing the 100 MHz picosecond laser source [41]. The measured modulation depth is 1.4%; however, the SA was not fully saturated due to the insufficient power of the laser source. The measured saturation intensity is 96.2 MW cm^{-2}. Nonsaturable losses are less than 37.8%. In comparison to previously described properties of GO paper [38], nonsaturable losses are reduced and saturation intensity and damage threshold are higher. The linear transmission spectra of SAs made from one to four layers of GO paper are presented in the inset of Fig. 7. The GO exhibits nearly wavelength-independent absorption in a wide range, which scales with the number of layers. The

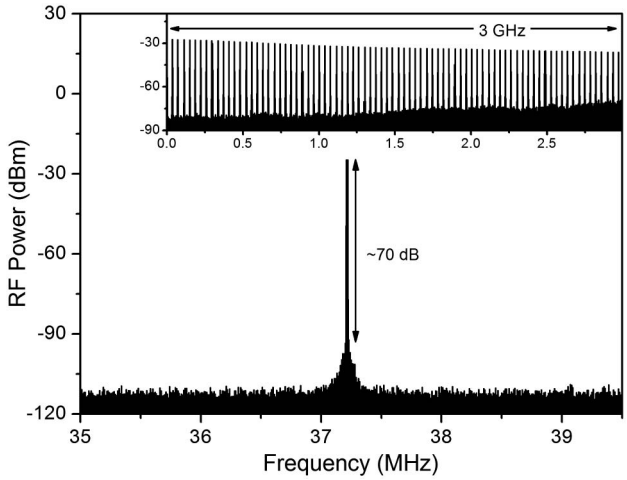

Fig. 6. Measured RF spectrum centered at a fundamental repetition frequency of 37.2 MHz and the spectrum measured with full available bandwidth (inset).

transmission level varies from 67% (for one layer), through 49% (for two layers), 44.7% (for three layers), to 29% (for four layers) at a 1550 nm wavelength. This measurement indicated that the thickness of the prepared GO paper is not entirely uniform.

An increasing number of GO paper layers causes an increase of the modulation depth. As confirmed by numerical simulations based on the extended nonlinear Schrödinger equation, the output pulse spectrum is broadening together with the increasing modulation depth of a SA, and temporal width tends to decrease simultaneously [42].

Table 1. Output Characteristics of Er-Doped Fiber Laser with up to Four Layers of GO Paper

No. of Layers	$\Delta\lambda_{FWHM}$ (nm)	λ_c (nm)	τ_{pulse} (fs)	TBP	P_{pump} (mW)	P_{out} (mW)	Peak Power (W)	E_{pulse} (pJ)	SNR (dB)
1	1.7	1565.9	1533	0.315	34.5	1.36	20.9	36.5	70
2	2.8	1561.9	913	0.315	38.0	0.89	23.0	23.9	71
3	3.7	1563.0	694	0.315	35.5	0.90	30.7	24.2	66
4	4.2	1564.4	613	0.315	34.5	0.83	32.0	22.3	69

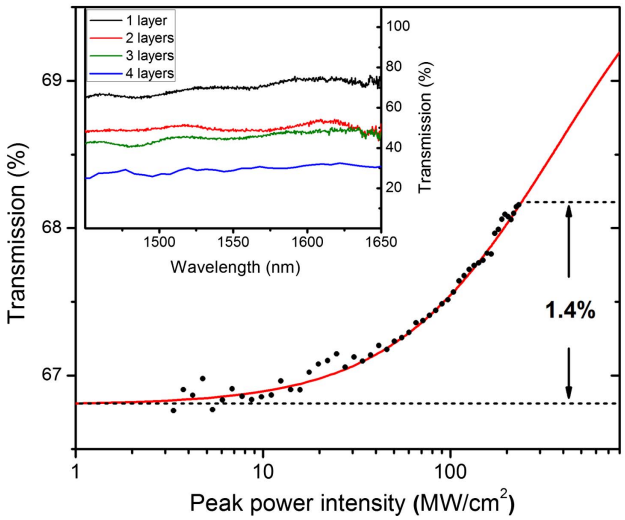

Fig. 7. Nonlinear transmission curve of GO paper SA. Inset: linear transmission spectra of GO-paper-based SAs made of one to four layers of GO paper.

B. Tm-Doped Fiber Laser

The experimental setup of a Tm-doped fiber laser is schematically presented in Fig. 8. The laser consists of a 1.5 m long active fiber (Nufern SM-TSF-9/125), a fiber isolator, an in-line polarization controller, a 20% output coupler, and a single-mode WDM. The laser was pumped with a 1565 nm laser diode, which was amplified in an Er/Yb-doped fiber amplifier (EYDFA). The GO-paper-based SA was formed similarly to the previous case. The laser performance was observed with the use of an optical spectrum analyzer (Yokogawa AQ6370B), an autocorrelator (Femtochrome FR-103XL), a RF spectrum analyzer (Agilent EXA N9010A), and a digital oscilloscope (Agilent Infiniium DSO91304A) connected to a fast photodiode.

Mode-locking operation starts at 98 mW of pumping power when the polarization controller is correctly set. All measurements were performed at 106 mW, where the best performance was observed. When the pump power exceeded 120 mW, higher harmonics and pulse breaking were noticed. The measured optical spectrum of generated pulses is presented in Fig. 9. The 4 nm FWHM band is centered at 1961.6 nm. In addition, characteristic dips originating from the water absorption lines in air can be seen in the spectrum [43]. The spectrum

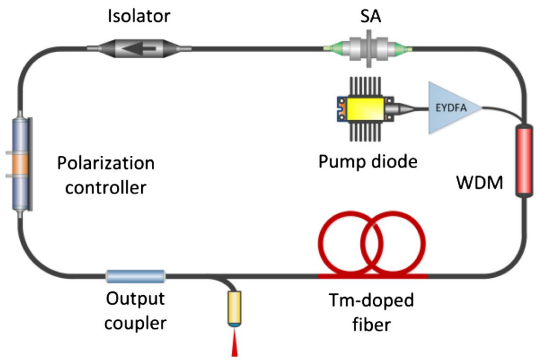

Fig. 8. Experimental setup of a Tm-doped fiber laser.

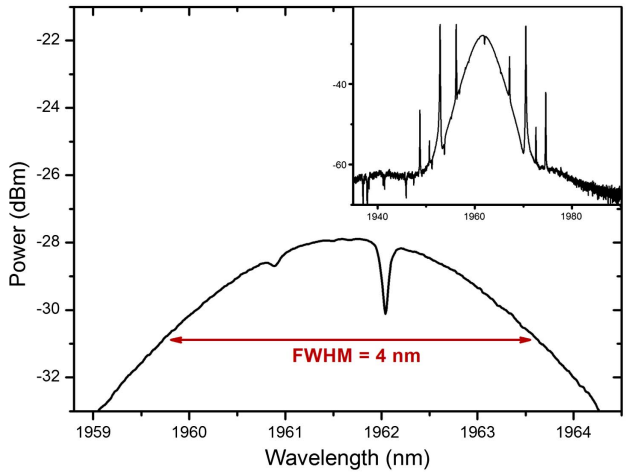

Fig. 9. Optical spectrum of the Tm-doped fiber laser.

has a typical soliton-like shape with strong, symmetrical Kelly's sidebands visible in the inset graph of the figure. The corresponding autocorrelation function is presented in Fig. 10(a). The pulse duration is 1.36 ps. The TBP of 0.424, compared with 0.315 for transform-limited pulses, indicates that the output pulse is about 25% longer than that resulting from the transform limit. The accumulated chirp originates from relatively high dispersion of the cavity and delivery fiber at the laser output in the 2 μm range. The linear transmission characteristic is depicted in Fig. 10(b). The transmission has a relatively flat profile with higher absorption for a longer wavelengths. The transmission is at the level of 30% at the central wavelength of laser emission.

The measured RF spectrum with a fundamental repetition rate of 27.37 MHz is presented in Fig. 10(c). The electrical SNR was approximately 80 dB. The stable RF spectrum recorded with full available bandwidth up to 3 GHz is depicted in the inset. The recorded oscilloscope pulse train is shown in Fig. 10(d). The cavity round-trip time is 36.5 ns, which coincides with a 7.12 m length of cavity. The output pulses are characterized by high amplitude stability.

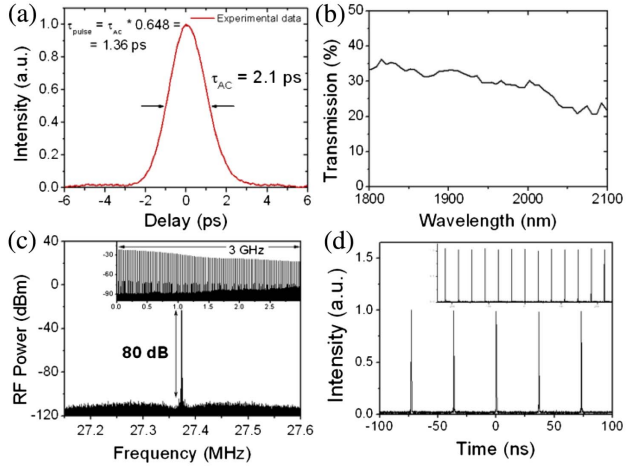

Fig. 10. (a) Autocorrelation trace of a 1.36 ps pulse generated in the Tm-doped fiber laser, (b) the linear transmission spectrum, (c) the fundamental repetition rate and RF spectrum in a 3 GHz span (inset) and (d) oscilloscope trace of output pulses.

4. CONCLUSIONS

We have demonstrated mode-locking operation of fiber lasers in both the 1.5 and 2 μm spectral ranges using the same GO paper in the role of SA. Owing to its flexibility, GO paper can be transferred onto a fiber connector to form the SA. Furthermore, GO shaped in the form of thin paper allows using more than one layer of the material. This enables control of the SA's parameters, and hence the output pulse characteristics, by increasing the number of GO paper layers. The FWHM of the optical spectrum might be scaled from 1.7 to 4.2 nm, corresponding to 1.5 ps and 613 fs pulse durations. The experiment was conducted on the example of an Er-doped fiber laser. In the case of a Tm-doped fiber laser, 1.36 ps solitons centered at 1961.9 nm pulses were achieved. Experiments showed that GO shaped in the form of a paper-like material may be considered for application as a SA in fiber lasers operating in various spectral ranges. The possibility of scaling the bandwidth of the optical spectrum and pulse duration is another advantage.

ACKNOWLEDGMENTS

The work presented in this article was supported by the Polish Ministry of Science and Higher Education under the project entitled "Investigation of saturable absorbers based on graphene oxide and reduced graphene oxide" (project no. IP2012 052072) and partially supported by the National Science Centre (NCN, Poland) under the project "Passive mode synchronization in fiber lasers based on low-dimensional materials—simulations and experiments" (decision no. DEC-2014/13/N/ST7/01968).

REFERENCES

1. U. Keller, "Recent developments in compact ultrafast lasers," Nature **424**, 831–838 (2003).
2. O. Okhotnikov, A. Grudinin, and M. Pessa, "Ultra-fast fibre laser systems based on SESAM technology: new horizons and applications," New J. Phys. **6**, 177 (2004).
3. K. Krzempek, G. Sobon, P. Kaczmarek, and K. M. Abramski, "A sub-100 fs stretched-pulse 205 MHz repetition rate passively mode-locked Er-doped all-fiber laser," Laser Phys. Lett. **10**, 105103 (2013).
4. S. Yamashita, Y. Inoue, S. Maruyama, Y. Murakami, H. Yaguchi, M. Jablonski, and S. Y. Set, "Saturable absorbers incorporating carbon nanotubes directly synthesized onto substrates and fibers and their application to mode-locked fiber lasers," Opt. Lett. **29**, 1581–1583 (2004).
5. G. Xing, H. Guo, X. Zhang, T. C. Sum, and C. H. A. Huan, "The physics of ultrafast saturable absorption in graphene," Opt. Express **18**, 4564–4573 (2010).
6. R. R. Nair, P. Blake, A. N. Grigorenko, K. S. Novoselov, T. J. Booth, T. Stauber, N. M. R. Peres, and A. K. Geim, "Fine structure constant defines visual transparency of graphene," Science **320**, 1308 (2008).
7. J. Ma, G. Xie, P. Lv, W. Gao, P. Yuan, L. Qian, U. Griebner, V. Petrov, H. Yu, H. Zhang, and J. Wang, "Wavelength- versatile graphene-gold film saturable absorber mirror for ultra-broadband mode-locking of bulk lasers," Sci. Rep. **4**, 5016 (2014).
8. L. M. Zhao, D. Y. Tang, H. Zhang, X. Wu, Q. Bao, and K. P. Loh, "Dissipative soliton operation of an ytterbium-doped fiber laser mode locked with atomic multilayer graphene," Opt. Lett. **35**, 3622–3624 (2010).
9. B. Fu, Y. Hua, X. Xiao, H. Zhu, Z. Sun, and C. Yang, "Broadband graphene saturable absorber for pulsed fiber lasers at 1, 1.5, and 2 μm," IEEE J. Sel. Top. Quantum Electron. **20**, 1100705 (2014).
10. H. Zhang, D. Tang, R. J. Knize, L. Zhao, Q. Bao, and K. P. Loh, "Graphene mode locked, wavelength-tunable, dissipative soliton fiber laser," Appl. Phys. Lett. **96**, 111112 (2010).
11. D. Popa, Z. Sun, F. Torrisi, T. Hasan, F. Wang, and A. C. Ferrari, "Sub 200 fs pulse generation from a graphene mode-locked fiber laser," Appl. Phys. Lett. **97**, 203106 (2010).
12. J. Sotor, G. Sobon, and K. M. Abramski, "Er-doped fibre laser mode-locked by mechanically exfoliated graphene saturable absorber," Opto-Electron. Rev. **20**, 362–366 (2012).
13. G. Sobon, J. Sotor, I. Pasternak, K. Grodecki, P. Paletko, W. Strupinski, Z. Jankiewicz, and K. M. Abramski, "Er-doped fiber laser mode-locked by CVD-graphene saturable absorber," J. Lightwave Technol. **30**, 2770–2775 (2012).
14. A. Martinez, K. Fuse, B. Xu, and S. Yamashita, "Optical deposition of graphene and carbon nanotubes in a fiber ferrule for passive mode-locked lasing," Opt. Express **18**, 23054–23061 (2010).
15. M. Zhang, E. J. R. Kelleher, F. Torrisi, Z. Sun, T. Hasan, D. Popa, F. Wang, A. C. Ferrari, S. V. Popov, and J. R. Taylor, "Tm-doped fiber laser mode-locked by graphene-polymer composite," Opt. Express **20**, 25077–25084 (2012).
16. G. Sobon, J. Sotor, I. Pasternak, A. Krajewska, W. Strupinski, and K. M. Abramski, "Thulium-doped all-fiber laser mode-locked by CVD-graphene/PMMA saturable absorber," Opt. Express **21**, 12797–12802 (2013).
17. Q. Wang, T. Chen, B. Zhang, M. Li, Y. Lu, and K. P. Chen, "All-fiber passively mode-locked thulium-doped fiber ring laser using optically deposited graphene saturable absorbers," Appl. Phys. Lett. **102**, 131117 (2013).
18. J. Sotor, G. Sobon, I. Pasternak, A. Krajewska, W. Strupinski, and K. M. Abramski, "Simultaneous mode-locking at 1565 nm and 1944 nm in fiber laser based on common graphene saturable absorber," Opt. Express **21**, 18994–19002 (2013).
19. J. Sotor, G. Sobon, J. Tarka, I. Pasternak, A. Krajewska, W. Strupinski, and K. M. Abramski, "Passive synchronization of erbium and thulium doped fiber mode-locked lasers enhanced by common graphene saturable absorber," Opt. Express **22**, 5536–5543 (2014).
20. M. Zhang, E. J. Kelleher, T. H. Runcorn, D. Popa, F. Torrisi, A. C. Ferrari, S. V. Popov, and J. R. Taylor, "Synchronously coupled fiber lasers and sum frequency generation using graphene composites," in *Conference on Lasers and Electro-Optics*, OSA Technical Digest (online) (Optical Society of America, 2014), paper STu1I.2.
21. H. He, J. Klinowski, M. Forster, and A. Lerf, "A new structural model for graphite oxide," Chem. Phys. Lett. **287**, 53–56 (1998).
22. Y. Zhu, S. Murali, W. Cai, X. Li, J. W. Suk, J. R. Potts, and R. S. Ruoff, "Graphene and graphene oxide: synthesis, properties and applications," Adv. Mater. **22**, 3906–3924 (2010).
23. X. Li, Y. Tang, Z. Yan, Y. Wang, B. Meng, G. Liang, H. Sun, X. Yu, Y. Zhang, X. Cheng, and Q. J. Wang, "Broadband saturable absorption of graphene oxide thin film and its application in pulsed fiber lasers," IEEE J. Sel. Top. Quantum Electron. **20**, 1101107 (2014).
24. Z. Liu, Y. Wang, X. Zhang, Y. Xu, Y. Chen, and J. Tian, "Nonlinear optical properties of graphene oxide in nanosecond and picosecond regimes," Appl. Phys. Lett. **94**, 021902 (2009).
25. X. H. Li, Y. G. Wang, Y. S. Wang, Y. Z. Zhang, K. Wu, P. P. Shum, X. Yu, Y. Zhang, and Q. J. Wang, "All-normal-dispersion passively mode-locked Yb-doped fiber ring laser based on graphene oxide saturable absorber," Laser Phys. Lett. **10**, 075108 (2013).
26. J. Xu, J. Liu, S. Wu, Q. H. Yang, and P. Wang, "Graphene oxide mode-locked femtosecond erbium-doped fiber lasers," Opt. Express **20**, 15474–15480 (2012).
27. J. Xu, S. Wu, H. Li, J. Liu, R. Sun, F. Tan, Q. H. Yang, and P. Wang, "Dissipative soliton generation from a graphene oxide mode-locked Er-doped fiber laser," Opt. Express **20**, 23653–23658 (2012).
28. G. Sobon, J. Sotor, J. Jagiello, R. Kozinski, M. Zdrojek, M. Holdynski, P. Paletko, J. Boguslawski, L. Lipinska, and K. M. Abramski, "Graphene oxide vs. reduced graphene oxide as saturable absorbers for Er-doped passively mode-locked fiber laser," Opt. Express **20**, 19463–19473 (2012).
29. Z. B. Liu, X. He, and D. N. Wang, "Passively mode-locked fiber laser based on a hollow-core photonic crystal fiber filled with

few-layered graphene oxide solution," Opt. Lett. **36**, 3024–3026 (2011).
30. M. Jung, J. Koo, P. Debnath, Y. W. Song, and J. H. Lee, "A mode-locked 1.91 μm fiber laser based on interaction between graphene oxide and evanescent field," Appl. Phys. Express **5**, 112702 (2012).
31. J. Lee, J. Koo, P. Debnath, Y.-W. Song, and J. H. Lee, "A *Q*-switched, mode-locked fiber laser using a graphene oxide-based polarization sensitive saturable absorber," Laser Phys. Lett. **10**, 035103 (2013).
32. H. Ahmad, A. Zulkifli, K. Thambiratnam, and S. Harun, "2.0 μm *Q*-switched thulium-doped fiber laser graphene oxide saturable absorber," IEEE Photon. J. **5**, 1501108 (2013).
33. J. Lee, J. Koo, Y. M. Jhon, and J. H. Lee, "Femtosecond harmonic mode-locking of a fiber laser based on a bulk-structured Bi_2Te_3 topological insulator," Opt. Express **23**, 6359–6369 (2015).
34. H. Zhang, S. B. Lu, J. Zheng, J. Du, S. C. Wen, D. Y. Tang, and K. P. Loh, "Molybdenum disulfide (MoS_2) as a broadband saturable absorber for ultra-fast photonics," Opt. Express **22**, 7249–7260 (2014).
35. D. A. Dikin, S. Stankovich, E. J. Zimney, R. D. Piner, G. H. B. Dommett, G. Evmenenko, S. T. Nguyen, and R. S. Ruoff, "Preparation and characterization of graphene oxide paper," Nature **448**, 457–460 (2007).
36. O. C. Compton and S. T. Nguyen, "Graphene oxide, highly reduced graphene oxide, and graphene: versatile building blocks for carbon-based materials," Small **6**, 711–723 (2010).
37. M. Ismail, H. Ahmad, and S. Harun, "Soliton mode-locked erbium-doped fiber laser using non-conductive graphene oxide paper," IEEE J. Quantum Electron. **50**, 85–87 (2014).
38. J. Boguslawski, J. Sotor, G. Sobon, R. Kozinski, K. Librant, J. Tarka, L. Lipinska, and K. M. Abramski, "Graphene oxide paper as a saturable absorber for Er-doped fiber laser," Proc. SPIE **9441**, 94410K (2014).
39. A. Jorio, M. Dresselhaus, R. Saito, and G. F. Dresselhaus, *Raman Spectroscopy in Graphene Related Systems* (Wiley-VCH, 2011).
40. L. Wang, J. Zhao, Y. Y. Sun, and S. B. Zhang, "Characteristics of Raman spectra for graphene oxide from ab initio simulations," J. Chem. Phys. **135**, 184503 (2011).
41. J. Du, Q. Wang, G. Jiang, C. Xu, C. Zhao, Y. Xiang, Y. Chen, S. Wen, and H. Zhang, "Ytterbium-doped fiber laser passively mode locked by few-layer molybdenum disulfide (MoS_2) saturable absorber functioned with evanescent field interaction," Sci. Rep. **4**, 6346 (2014).
42. J. Jeon, J. Lee, and J. H. Lee, "Numerical study on the minimum modulation depth of a saturable absorber for stable fiber laser mode locking," J. Opt. Soc. Am. B **32**, 31–37 (2015).
43. L. S. Rothman, I. E. Gordon, A. Barbe, D. C. Benner, P. E. Bernath, M. Birk, V. Boudon, L. R. Brown, A. Campargue, J. P. Champion, K. Chance, L. H. Coudert, V. Dana, V. M. Devi, S. Fally, J. M. Flaud, R. R. Gamache, A. Goldman, D. Jacquemart, I. Kleiner, N. Lacome, W. J. Lafferty, J. Y. Mandin, S. T. Massie, S. N. Mikhailenko, C. E. Miller, N. Moazzen-Ahmadi, O. V. Naumenko, A. V. Nikitin, J. Orphal, V. I. Perevalov, A. Perrin, A. Predoi-Cross, C. P. Rinsland, M. Rotger, M. Simeckova, M. A. H. Smith, K. Sung, S. A. Tashkun, J. Tennyson, R. A. Toth, A. C. Vandaele, and J. Vander Auwera, "The HITRAN 2008 molecular spectroscopic database," J. Quant. Spectrosc. Radiat. Transfer **110**, 533–572 (2009).